

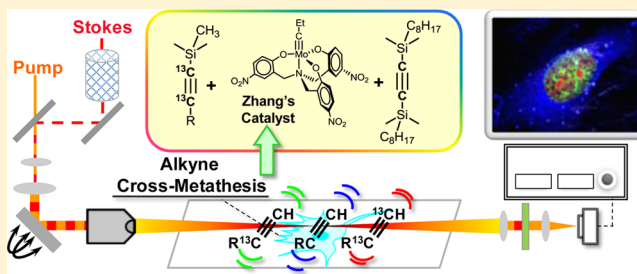
Multicolor Live-Cell Chemical Imaging by Isotopically Edited Alkyne Vibrational Palette

Zhixing Chen,[†] Daniel W. Paley,[†] Lu Wei,[†] Andrew L. Weisman,[‡] Richard A. Friesner,[†] Colin Nuckolls,^{*,†} and Wei Min^{*,†,§}

[†]Department of Chemistry, [‡]Department of Applied Physics and Applied Mathematics, and [§]Kavli Institute for Brain Science, Columbia University, New York, New York 10027, United States

Supporting Information

ABSTRACT: Vibrational imaging such as Raman microscopy is a powerful technique for visualizing a variety of molecules in live cells and tissues with chemical contrast. Going beyond the conventional label-free modality, recent advance of coupling alkyne vibrational tags with stimulated Raman scattering microscopy paves the way for imaging a wide spectrum of alkyne-labeled small biomolecules with superb sensitivity, specificity, resolution, biocompatibility, and minimal perturbation. Unfortunately, the currently available alkyne tag only processes a single vibrational “color”, which prohibits multiplex chemical imaging of small molecules in a way that is being routinely practiced in fluorescence microscopy. Herein we develop a three-color vibrational palette of alkyne tags using a ¹³C-based isotopic editing strategy. We first synthesized ¹³C isotopologues of EdU, a DNA metabolic reporter, by using the newly developed alkyne cross-metathesis reaction. Consistent with theoretical predictions, the mono-¹³C (¹³C≡¹²C) and bis-¹³C (¹³C≡¹³C) labeled alkyne isotopologues display Raman peaks that are red-shifted and spectrally resolved from the originally unlabeled (¹²C≡¹²C) alkynyl probe. We further demonstrated three-color chemical imaging of nascent DNA, RNA, and newly uptaken fatty-acid in live mammalian cells with a simultaneous treatment of three different isotopically edited alkynyl metabolic reporters. The alkyne vibrational palette presented here thus opens up multicolor imaging of small biomolecules, enlightening a new dimension of chemical imaging.



INTRODUCTION

Advances in optical microscopy in the past decades have revolutionized the way modern biological sciences are conducted. In particular, powerful fluorescence imaging techniques have flourished, largely driven by the advent of a diversity of fluorescent probes including organic dyes,¹ genetically encoded fluorescent proteins,² and semiconductor quantum dots.³ A recurring theme in all these exciting developments is the creation of a palette of multiple colors resolvable from each other in the visible spectrum. Through targeting several species of interest simultaneously, these palette sets have enabled multiplex studies for visualization, localization, and interaction in a broad spectrum of structural and functional assays. Notable applications include protein–protein interactions by FRET between different fluorescent proteins or organic dyes,⁴ super-resolution structural imaging by multicolor STED,⁵ and PALM/STORM⁶ as well as functional imaging using palettes of calcium-sensitive proteins⁷ and voltage-sensitive dyes.⁸ However, fluorescent probes are not suitable for tagging small biomolecules (e.g., nucleic acids, amino acids, fatty acids), because the relatively bulky fluorescent tags (even the smallest dyes) often destroy or significantly alter the biological activities of small biomolecules.

Raman-based vibrational microscopy represents an alternative to fluorescence microscopy. Raman microscopy is well

suited for probing small biomolecules, especially when coupled with specific, small-size vibrational tags. Among the existing vibrational tags such as bioorthogonal chemical moieties or stable isotopes,⁹ alkynes are unique due to a combination of several merits including its small size (two atoms), high Raman activity of C≡C stretching, and a signal frequency well separated from endogenous cellular background. Bioimaging using alkyne tags was initially demonstrated with 5-ethynyldeoxyuridine (EdU), a cell-proliferation reporter, and other mobile molecules by conventional spontaneous Raman microscopy.^{10,11} Very recently, our group has coupled alkyne tags with stimulated Raman scattering (SRS) microscopy as a general strategy for imaging small biomolecules¹² (Figure 1a). Compared to the spontaneous counterpart, SRS is a state-of-the-art chemical imaging technique offering: substantial signal amplification, sensitivity increases, speed acceleration, immunity to autofluorescence, and optical penetration and sectioning in 3D tissues and whole animals.^{13–16} As such, we have achieved visualizing metabolic incorporation of alkyne-tagged small precursors of deoxyribonucleoside, ribonucleoside, amino acid, choline, and fatty acid into newly synthesized DNA, RNA, proteomes, phospholipids, and triglycerides, respectively, in live

Received: March 17, 2014

Published: May 21, 2014

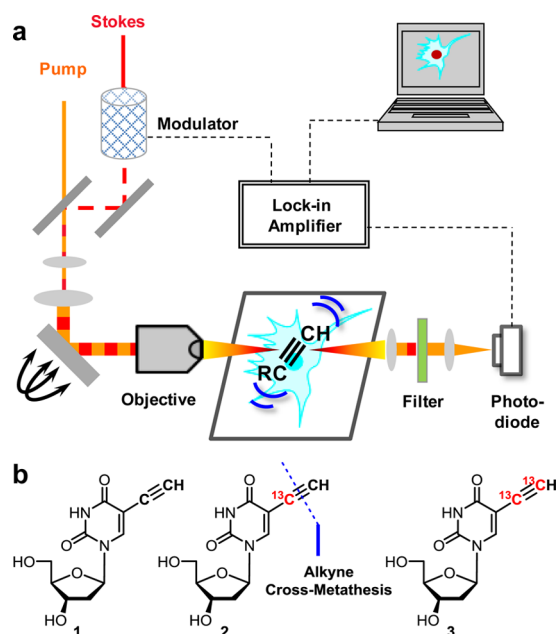


Figure 1. Isotopically edited alkyne vibrational tags for chemical imaging by SRS microscopy. (a) Setup of SRS microscope for alkyne vibrational imaging. When the energy difference between the pump and the Stokes photons matches with the alkyne vibration mode, their joint action will greatly accelerate the vibrational excitation of alkyne bonds. As a result of energy exchange between the input photons with the alkynes, the output pump and Stokes beams will experience intensity loss and intensity gain, respectively. Such intensity changes measured by SRS microscope generate concentration-dependent alkyne distributions in 3D. (b) Structures of unlabeled, mono, and bis ^{13}C -labeled 5-ethynyl-2'-deoxyuridine (EdU). Mono- ^{13}C -labeled EdU, **2**, is retrosynthetically disconnected using alkyne cross-metathesis chemistry.

cells and organisms, and tracking 3D delivery of an alkyne-bearing drug in mouse skin tissue.¹²

In terms of specific labeling and detection, Raman imaging of alkyne-tagged small biomolecules is conceptually analogous to fluorescence imaging of fluorophore (including dyes, proteins, and quantum dots) labeled larger species. However, unlike its fluorescence counterpart, multicolor Raman imaging of alkyne-tagged molecules lacks a general solution. The Raman vibrational frequencies of alkynyl molecules, located in a spectral region between 2080 and 2260 cm^{-1} , depend on the chemical structures and are not easily subject to customization. Examples of dual-color Raman imaging of alkyne-tagged molecules have been demonstrated using two structurally different alkynyl probes in which the electronic or conjugation properties of the triple bonds render resolvable Raman peaks.^{11,12} However, Raman peaks of most of typical alkynyl probes still overlap with each other. Therefore, the prefixed Raman frequencies of alkyne-tagged molecules prevent multiplexed chemical imaging of small molecules in a general way that is being routinely practiced in fluorescence microscopy.

The study reported here reveals a general chemical strategy to expand the vibrational palette of terminal alkyne tags. Inspired by classical isotope approaches adapted for vibrational spectroscopy,^{17–22} we envision that introduction of one or two heavy ^{13}C atom(s) into the alkynyl group would dampen the original stretching frequency of the $^{12}\text{C}\equiv^{12}\text{C}$ bond and thus create new vibrational “colors”. To address the underlying synthetic challenge, we show here the preparation of three

distinct forms of ^{13}C isotopically edited alkyne vibrational tags by using the newly developed alkyne cross-metathesis chemistry.²³ The three forms of alkynes ($^{12}\text{C}\equiv^{12}\text{C}$; $^{13}\text{C}\equiv^{12}\text{C}$; $^{13}\text{C}\equiv^{13}\text{C}$) are biochemically identical and, to our delight, display three mutually resolvable Raman peaks. We demonstrate three-color SRS imaging of DNA, RNA, and lipid metabolism using three different alkyne-tagged small-molecule metabolic reporters in live mammalian cells. Thus, our isotopic editing approach for creating alkyne palettes paves the way for multicolor chemical imaging, bringing small biomolecules under the illumination of modern light microscopy.

RESULTS

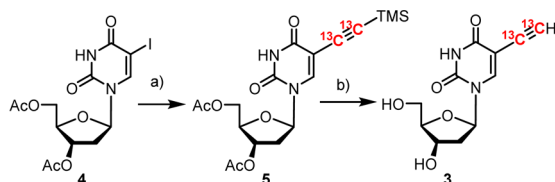
Theoretical Consideration of Raman Spectra. We first seek for some theoretical insights by using a simple classical mechanics model. The wavenumber of an alkyne stretching oscillation, $\bar{\nu}$, is related to the force constant of the triple bond (k) as well as the mass of the two carbons (m_1 and m_2) using Hooke's law:

$$\bar{\nu} = \frac{1}{2\pi c} \sqrt{\frac{k}{\mu}}, \quad \text{where } \mu = \frac{m_1 m_2}{m_1 + m_2} \quad (1)$$

For a typical alkyne ($\bar{\nu} = 2125 \text{ cm}^{-1}$), if one of the alkyne carbons is substituted by ^{13}C , the wavenumber of the stretching vibration is calculated to be 2084 cm^{-1} , assuming the change in the bond strength is negligible. Likewise, bis- ^{13}C -labeled alkyne has a predicted wavenumber of 2042 cm^{-1} . Therefore, the expected spectral shifts of mono- and bis-isotopically labeled alkyne are 41 and 83 cm^{-1} , respectively.

In order to obtain a more accurate prediction, we further calculated the frequencies for the triple-bond stretching using density functional theory (DFT) at the B3LYP/6-31G* level of theory with the scaled quantum mechanical force field method.²⁴ We use 5-ethynyl-2'-deoxyuridine (EdU, **1**) and its isotopologues, EdU- ^{13}C (**2**) and EdU- $^{13}\text{C}_2$ (**3**), as model compounds (Figure 1b). EdU is a thymidine analogue that incorporates into newly synthesized DNA and is typically detected by fluorescent labeling via click chemistry.²⁵ We use EdU as a model alkynyl vibrational probe as it is the first reported alkyne-tagged molecule imaged with Raman microscopy.¹⁰ The DFT-calculated vibrational frequencies for isotopically edited EdUs are 2126 cm^{-1} (for **1**), 2076 cm^{-1} (for **2**), and 2051 cm^{-1} (for **3**). Given that the Raman peaks due to alkyne stretching are intrinsically sharp (typical fwhm = 14 cm^{-1}),¹² the ^{13}C isotope editing strategy should afford three spectroscopically resolvable alkyne vibrational tags for live cell Raman imaging and analysis.

Synthesis of Isotopically Edited EdUs. Encouraged by the theoretical predictions above, we developed chemical synthesis of the isotopically edited EdUs. Despite the commercial availability of EdU- $^{12}\text{C}_2$ (**1**), its isotopologues, EdU- ^{13}C (**2**) and EdU- $^{13}\text{C}_2$ (**3**), need to be chemically synthesized for characterization. EdU is prepared by alkynylation of 5-iododeoxyuridine by a Sonagashira coupling.²⁶ We used an analogous method in which acetylated 5-iododeoxyuridine (**4**) was subjected to Sonagashira coupling with trimethylsilylacetylene- $^{13}\text{C}_2$ to yield intermediate **5** (Scheme 1). Global deprotection with K_2CO_3 affords EdU- $^{13}\text{C}_2$ (**3**). However, the mono- ^{13}C -labeled EdU (**2**) is a synthetic challenge due to the difficulty in creating the $^{13}\text{C}_1$ alkynyl building block.

Scheme 1. Synthesis of 3 by Sonagashira Coupling^a

^aReagents and conditions: (a) Pd(OAc)₂ (10% mol), PPh₃ (20% mol), CuI (10% mol), Et₃N (3.0 equiv), and TMS¹³C≡¹³CH (1.5 equiv), DMF, RT, 15 h, 72%; (b) K₂CO₃ (5.0 equiv), MeOH/H₂O, RT, o/n, 75%.

We reasoned that an alkyne cross-metathesis disconnection would provide direct access to the mono-¹³C-labeled alkyne from EdU-¹³C₂ (3). Alkyne metathesis^{27,28} is emerging as a viable tool for synthesis of complex molecules such as natural products and polymers. These advances are enabled by the development of new generations of catalysts that have higher catalytic activity and broader substrate compatibility.²³ Nevertheless, alkyne metathesis, especially cross-metathesis, had not been demonstrated on chemical biology reporters with a myriad of functional groups. Since metathesis of terminal alkynes remains a challenge,²⁹ we turned to the TMS protected 5 as the substrate for metathesis.³⁰ It should be noted that TMS-protected alkynes exhibit reduced reactivity compared to typical internal alkynes.³¹

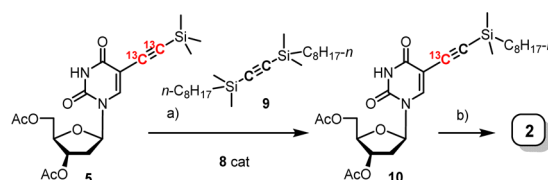
We initially planned to metathesize 5 with a large excess (100 equiv) of bis(trimethylsilyl)acetylene, 6, as the isotopic editing reagent to achieve a theoretical 99.5% conversion to mono-¹³C-5 at equilibrium. We first evaluated the commercially available Schrock catalyst³² (7) for alkyne metathesis (Table 1). Reacting 5 with 5 equiv of 6 and 100 equiv of 7 gave no conversion at room temperature (entry 1). When heated to 80 °C, a side product was obtained (entry 2, see Supporting Information for detail), indicating that the glycosylamine was not compatible with the tungsten catalyst.³³ Therefore, we switched to a newly

Table 1. Investigation of Conditions for the Alkyne Cross-Metathesis

entry	catalyst, equiv	6 loading, equiv	temp.	time, h	yield	5a:5
1	7, 5	100	RT	12	N/R	
2	7, 5	100	80 °C	12	side product	
3	8, 5	100	RT	12	N/R	
4	8, 5	100	80 °C	12	20%	2.2:1
5	8, 0.5	10	80 °C	12	N/R	

engineered podand-supported molybdenum catalyst (8) with high catalytic activity and stability developed by Zhang and Jyothish.³⁴ Substrate 5 is still inert to metathesis with 6 in the presence of catalyst 8 at room temperature (entry 3), but at 80 °C the reaction yields an inseparable 2.2:1 mixture of metathesis product and unreacted starting material, along with uncharacterized byproducts (entry 4). Reducing the catalyst loading and the equivalence of 6 fails to yield 5 (entry 5), indicating that a high concentration of alkyne is required to drive the reaction of this relatively sterically encumbered substrate.

Based on these results, we decided not to search for another protocol to push the conversion of the bulky substrate to >95%. Instead, we developed an alternative strategy to separate the mono-¹³C product from unreacted starting material (Scheme 2). We reason that a different protecting group from TMS,

Scheme 2. Synthesis of 2 by Alkyne Cross-Metathesis^a

^aReagents and conditions: (a) 9 (100 equiv), 8 (5 equiv), CCl₄, 70 °C, 8 h, 27%, 33% BRSM; (b) K₂CO₃, TBAF, MeOH/H₂O, RT, 7 h, 50%.

once introduced to the product, would render the product isolable by chromatography. We chose octyldimethylsilyl as it is more hydrophobic than the TMS group but not too bulky to inhibit the reaction. We prepared bis(octyldimethylsilyl)-acetylene (9) and metathesized 5 with 9 in the presence of 8. To our delight, the desired product, compound 10, was isolated in pure form in a moderate yield (33% based on recovered starting materials). Deprotection with K₂CO₃ and TBAF afforded the final product, EdU-¹³C (2). The isotopic features of 2 and 3 are characterized by mass spectrometry and ¹H NMR and by the coupling between ¹³C and ¹H (see Supporting Information for detail).

Characterization of Multicolor Alkyne Vibrational Tags by Raman Spectroscopy and SRS Imaging. With compounds 1–3 in hand, we first measured their Raman spectroscopic properties as labeling reagents for *de novo* DNA synthesis in proliferating cells. HeLa cells were treated with 0.1 mM of 1, 2, and 3, respectively, for 15 h, then fixed, and analyzed using a Raman microspectrometer. The three isotopologues are all biochemically active, as alkyne stretching peaks are detectable in the cell nuclei of all three samples (Figure 2). Incorporated EdU (1) exhibits a Raman peak at 2125 cm⁻¹ as expected, while incorporated EdU-¹³C (2) and EdU-¹³C₂ (3) have displayed markedly shifted peaks at 2077 and 2048 cm⁻¹, respectively. Therefore, the central wave-numbers of the measured new peaks are in good agreement with the DFT predictions (2076 and 2051 cm⁻¹). More importantly, thanks to the intrinsic sharpness (typical fwhm = 14 cm⁻¹) of alkyne peaks, the spectral shifts of EdU-¹³C (2) and EdU-¹³C₂ (3) are just large enough so that all three peaks are completely resolved from each other.

We next evaluated compounds 1–3 in live mammalian cells under SRS microscopy (Figure 3). In our SRS microscope setup, the pulse widths of both pump and Stokes lasers are set to 6 ps, corresponding to an excitation profile of 6 cm⁻¹. This

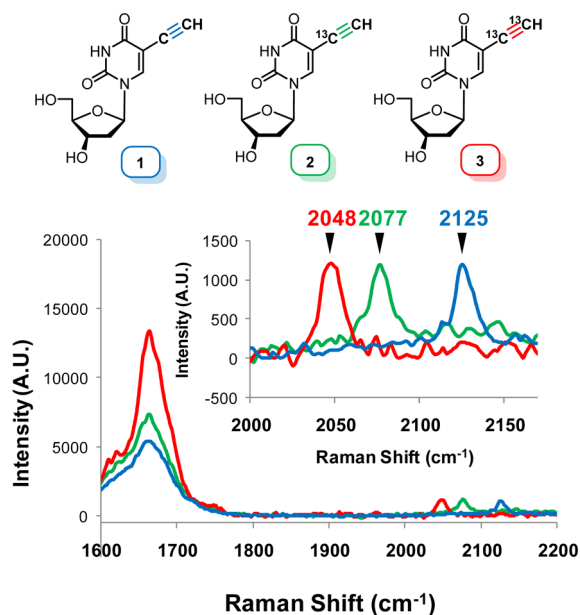


Figure 2. Raman spectra of HeLa cells incubated with three isotopically edited EdUs. Spectra are acquired from nucleus region of fixed cells after incubation with either 1, 2, or 3. Amide bond stretchings at 1655 cm^{-1} are shown as reference. The spectra are normalized according to the alkyne peak. Inset: enlarged Raman spectra from 2000 to 2170 cm^{-1} .

excitation profile is slightly narrower than 14 cm^{-1} (fwhm) of alkyne peaks, rendering both an efficient and a selective SRS excitation to the specifically labeled alkynes.¹² To test the orthogonality of 1–3, live HeLa cells treated with each probe were imaged under all five channels: 1655 (amide channel, total protein), 2000 (off-resonance channel), 2048 , 2077 , and 2125 cm^{-1} (on-resonance channels with the three alkyne peaks, respectively). Images are acquired sequentially under the same laser powers. As shown in Figure 3, for EdU (1), a prominent signal is observed at the 2125 cm^{-1} on-resonance channel, depicting the newly synthesized DNA inside nucleus. In contrast, the 2000 , 2048 , and 2077 cm^{-1} channels detect only weak and dispersive background which may be attributed to optical cross-phase modulations.³⁵ Similarly, when using

EdU- ^{13}C (2) or EdU- $^{13}\text{C}_2$ (3) as the probe, DNA synthesis signals are only detected at the corresponding on-resonance channel of 2077 or 2048 cm^{-1} (Figure 3). These SRS images, along with the spectroscopic data, unambiguously prove isotopic editing as a viable strategy of spectral shifting for multichannel Raman study of alkyne-tagged molecules.

Three-Color SRS Imaging of Isotopic Alkyne Vibrational Tags. Currently, there exists a variety of alkyne derivatized metabolic labeling reagents for studying DNA, RNA, proteins, lipids, and other biomolecules.³⁶ These probes were developed originally for the subsequent Cu-catalyzed click reactions³⁷ but have proven to be also suitable for direct Raman imaging.¹² We choose three well-documented alkynyl reporters for our demonstration: ethynyluridine (EU, 11) as a small-molecule precursor for RNA synthesis,³⁸ 17-octadecynoic acid (17-ODYA, 12) as a lipid precursor as well as a protein post-translational modification reagent³⁹ and EdU (1) for DNA synthesis. As shown in Figure 4a, the Raman spectra of EU (11, aqueous solution), EdU (1, aqueous solution), and 17-ODYA (12, neat) exhibit peaks at 2126 , 2123 , and 2120 cm^{-1} , respectively. The near complete spectral overlap among the three Raman peaks is thus prohibitive for further attempts of multicolor imaging.

Enlightened by the isotopic editing concept, we used the mono- ^{13}C -labeled EdU- ^{13}C (2), a bis- ^{13}C -labeled EU- $^{13}\text{C}_2$ (13) and 17-ODYA (12) to address this issue. We first verified the Raman spectra of the isotopically edited probes as shown in Figure 4b. In aqueous solutions, EU- $^{13}\text{C}_2$ (13, see Supporting Information for synthesis) has a shifted peak at 2053 cm^{-1} , which is well-resolved from the 2077 cm^{-1} peak of EdU- ^{13}C (2, aqueous solution) and the 2120 cm^{-1} peak of 17-ODYA (12). Therefore, we moved on to test the three-color live cell SRS imaging of RNA, DNA, and lipid metabolism using EU- $^{13}\text{C}_2$ (13), EdU- ^{13}C (2), and 17-ODYA (12).

HeLa cells were treated with 13, 2, and 12 simultaneously before being imaged by SRS microscopy. Two living cells are captured in Figure 4c. In the 2053 cm^{-1} channel, the signal for total RNA is observed mainly inside the nucleus of both cells, with intense signal at nucleoli where rRNA assembly takes place. In the 2077 cm^{-1} channel, the EdU- ^{13}C signal shows a nuclear distribution of newly synthesized DNA in one cell but not the other (indicating different cell cycle status). In the 2125

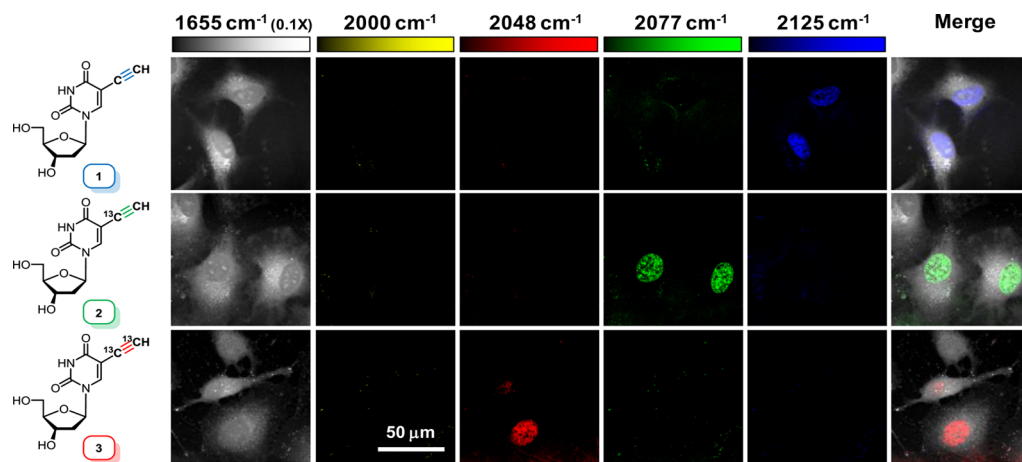


Figure 3. Live cell SRS imaging of DNA synthesis in HeLa cells incubated with isotopically edited EdUs. For each sample incubated with either 1, 2, or 3, images are acquired in 5 different Raman channels: 1655 (amide bond), 2000 (off-resonant), 2048 (on-resonant with 3), 2077 (on-resonant with 2), and 2125 cm^{-1} (on-resonant with 1) in sequential mode. Images are acquired in 512×512 pixels with a pixel dwell time of $40\text{ }\mu\text{s}$.

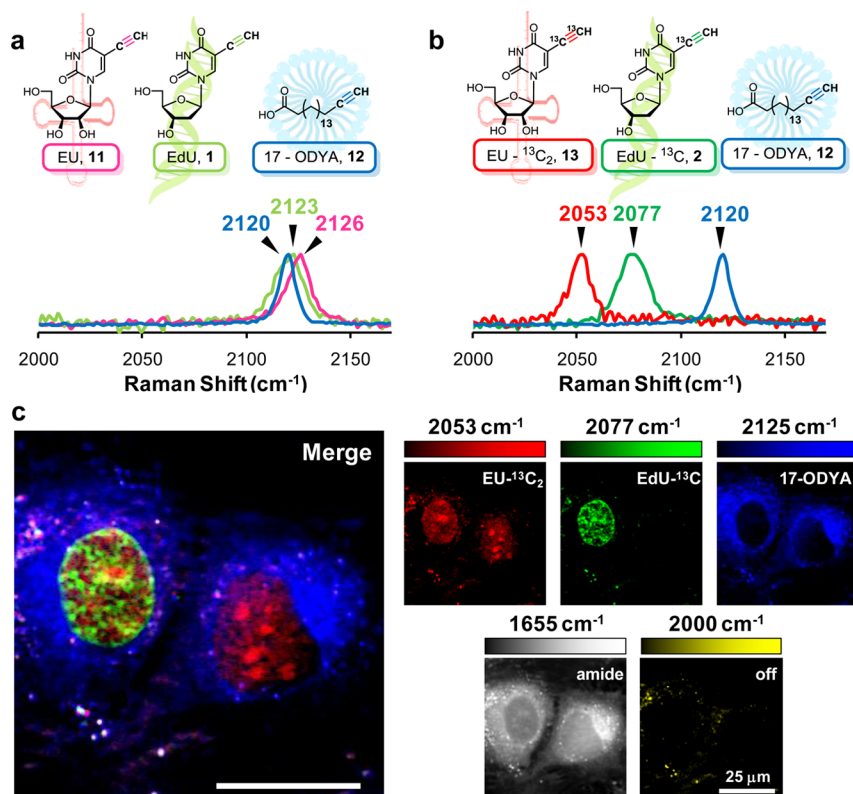


Figure 4. Three-color chemical imaging using isotopically edited alkyne tags. (a) Structures and normalized Raman spectra of RNA probe EU (11), DNA probe EdU (1), and fatty acid probe 17-octadecynoic acid (12). (b) Structures and normalized Raman spectra of isotopically edited EU- $^{13}\text{C}_2$ (13), EdU- ^{13}C (2), and 17-ODYA (12). (c) Three-color SRS imaging of nascent RNA, DNA, and fatty acyl derivatives in live HeLa cells by spectral targeting of different isotopically edited alkyne tags. Images are acquired in 5 different Raman channels: 1655 (amide bond), 2000 (off-resonant), 2053 (on-resonant with 13), 2077 (on-resonant with 2), and 2125 cm^{-1} (on-resonant with 12) in sequential mode. Images are acquired in 341×341 pixels with a pixel dwell time of 40 μs .

cm^{-1} channel, the signal is derived from 17-ODYA (12) incorporation to lipids that exhibit cytosolic localization. These observations are in accordance with the known cell biology that DNA replication happens only when cells are progressing through the S phase while fatty acid take-up and RNA synthesis processes are less dependent on cell cycles. Little background is observed in the 2000 cm^{-1} off-resonance channel. Amide channel at 1655 cm^{-1} , interpreted as total protein signal, is shown as a reference. In the final merged image of Figure 4c, three alkynyl molecules could be differentiated unambiguously, allowing for multiplex studies of colocalization and interactions.

Overall, by introducing isotopically edited alkyne tags we have successfully rendered different alkynyl metabolic probes three distinctive Raman “colors”. This approach could be readily applied to studying other combinations of small-molecule reporters. It is noteworthy that the live-cell three-color Raman imaging of isotopic alkyne-tagged metabolic reporters demonstrated here would be difficult to achieve otherwise, e.g., by using fluorescent reporters due to the limited choices of bioorthogonal chemistry.

DISCUSSION

Our spectroscopic and imaging studies demonstrate that the mono- and bis- ^{13}C isotopically barcoded alkyne tags can shift Raman peaks to be well resolved from their unmodified counterpart. This isotopic editing strategy has enabled us to perform live cell three-color chemical imaging of DNA, RNA, and fatty-acid metabolism simultaneously, by three ethynyl-

derivatized reporters: EU- $^{13}\text{C}_2$, EdU- ^{13}C , and 17-ODYA. Impressively, EdU- ^{13}C was prepared via an alkyne cross-metathesis reaction using a podand-supported molybdenum(VI) catalyst.³⁴ Alkyne vibrational tags can now be employed in three mutually orthogonal versions as reporters for high-resolution, multicolor chemical imaging and subsequent studies on spatial colocalization and functional interactions. This work thus represents important progress toward chemical imaging of complex biological processes in live cells.

From a synthetic chemistry point of view, this work is not only a rare demonstration of preparing a bioprobe using alkyne metathesis but also one of the few examples in which relatively bulky (trialkylsilyl)alkynes are subjected to cross-metathesis. Notably, the molybdenum catalyst used here is mild enough for the sensitive hemiaminal ether structure of EdU. Considering that the metathesis of TMS-protected alkyne was proposed³⁰ in 1983 and first demonstrated³¹ in 2001, it is clear that the evolution of catalysts has been constantly broadening the scope of alkyne metathesis. We expect that, with the development of milder and more active catalysts,^{40,41} alkyne metathesis would be carried out under mild conditions with higher yields. As progress has been made on metathesizing unprotected terminal alkynes²⁹ and on alkyne metathesis in protic media,⁴² the work reported here will be regarded not only as an early effort of using alkyne metathesis in the preparation of bioimaging reagent but also as a prelude of alkyne metathesis as a general tool in bioconjugation and bio-orthogonal chemistry.⁴³

From an isotopic chemistry point of view, this work reaffirms the unique role of isotopes in vibrational spectroscopy. While

fluorescent dyes and proteins change their color by modulating the delocalization of conjugated π electrons and quantum dots by quantum confinement effects, alkyne vibrational palette harness the fundamental mass-energy relation to tune the vibrational frequency. Indeed, isotopic editing has been broadly applied in chemistry studies including multicolor Raman imaging of ^{13}C -doped carbon nanotubes,¹⁷ studying β -sheet structure with ^{13}C -labeled carbonyls as infrared (IR) probes,¹⁸ characterizing single-molecule surface-enhanced Raman spectroscopy,^{19,20} and tuning spectroscopic profiles of environmentally sensitive IR probes.^{21,22} By overcoming the synthetic hurdle via alkyne metathesis, here we have achieved the isotopic editing of alkynes. It is also noteworthy that two-color alkyne imaging could be occasionally achieved in rare cases when molecules have resolvable Raman shifts (e.g., propargylcholine having a shifted Raman peak presumably due to a nearby positive charge,¹² or by introducing other bulkier groups such as diynes¹¹). Isotopic editing, however, offers a general and modular way to change Raman peaks of alkynyl molecules. On a broader perspective, the isotopically edited alkynyl molecules could be further used in modalities beyond vibrational imaging, like MRI⁴⁴ and mass-spec based imaging/analysis.⁴⁵

From a Raman imaging instrumentation point of view, the SRS images in this work are recorded at a pixel dwell time of 40 μs , ~ 4500 times faster than in a spontaneous Raman imaging setup.¹⁰ Nevertheless, isotopically edited alkynes should also be applicable to more accessible spontaneous Raman microscopes, which requires longer time to reconstruct an image but offers a full spectrum at each pixel.^{46,47} Moreover, the SRS microscope setup in this work could be further upgraded toward advanced multicolor imaging applications with alkyne vibrational tags. First, higher stimulated Raman loss signal could be achieved by equipping stronger lasers, i.e., fiber lasers, rendering more sensitive detections of alkynyl molecules.⁴⁸ Second, the background signal derived from cross-phase modulation could be reduced by a recently reported spectral modulation technique.⁴⁹ Lastly, the newly developed rapidly tunable optical parametric oscillator would enable line-by-line acquisition of multicolor SRS images, which would reduce the potential artifacts caused by sample motions in current frame-by-frame imaging acquisition mode.⁵⁰

From an imaging probe point of view, the alkyne vibrational palette described here adds to a new dimension of imaging reagents for studying metabolically labeled biomolecules as well as nonimmobilized cellular small molecules. In comparison, fluorescence-based methods of imaging metabolically labeled biomolecules largely rely on Cu-catalyzed click chemistry on fixed samples.³⁶ The development of Cu-free click chemistry is, while fast,^{51–53} still limited to few functional groups such as cyclooctyne⁵⁴ and tetrazine.⁵⁵ Therefore, the alkyne vibrational tags, now available in three colors, represent a major advantage. Finally, the isotopic alkyne-tagged molecules would retain their click-chemistry reactivity with subsequent biochemical pull-down reagents, rendering a combination of complementary methods on different levels.

CONCLUSION

We present the isotopic editing of alkyne vibrational tags: the theory-guided design, chemical synthesis via alkyne metathesis, spectroscopic characterization, and their application in three-color live-cell chemical imaging using SRS microscopy. The alkyne vibrational palette offers a new dimension to multicolor chemical imaging, complementing fluorescence microscopy in

multiplex studies for visualization, localization, and interaction of a variety of biochemical species in live cells. Moreover, the strategic application of alkyne cross-metathesis in the chemical synthesis of isotopic barcodes echoes the impact of emerging synthetic methodology to the development of chemical reporters for burgeoning bioimaging applications.

METHODS

SRS Microscopy. The microscopy set up was previously described.¹² Briefly, an integrated light source (picoEMERALD with custom modification, Applied Physics & Electronics, Inc.), consisting of a Stokes beam (1064 nm, 6 ps, 80 MHz repetition rate) modulated at 8 MHz and a spatially- temporally overlapping pump beam (tunable, 720–990 nm, 5–6 ps, 80 MHz repetition rate) is coupled into an inverted multiphoton laser-scanning microscope (FV1200MPE, Olympus). Lasers are delivered to the cell samples through a 60 \times water objective (UPlanAPO/IR, 1.2 N.A., Olympus) and then collected with a condenser lens (oil immersion, 1.4 N.A., Olympus). The Stokes beam is then blocked with a high O.D. bandpass filter (890/220 CARS, Chroma Technology), while the pump beam is imaged onto a Si photodiode (FDS1010, Thorlabs). To detect the stimulated Raman loss, output current from the Si photodiode is terminated, filtered, and demodulated using a lock-in amplifier (SR844; Stanford Research Systems). The output of the lock-in amplifier is sent to the microscope through an analogue interface box (FV10-ANALOG, Olympus), and images are reconstructed using Fluoview software (Olympus). The imaging experiments in this study are performed with 168 mW pump beam and 134 mW Stokes beam (power measured after objective). Images are acquired with a 40 μs pixel dwell time and a 10 μs time constant from the lock-in amplifier. For multichannel SRS experiments, images are acquired in sequential mode with a laser tuning duration of 40–80 s between channels. The total acquisition time of a 5 channel SRS image is 5 min.

Raman Spectroscopy. Raman spectra were acquired at room temperature with a Raman spectrometer (inVia Raman microscope; Renishaw) equipped with a 532 nm diode laser through a 50 \times , 0.75 N.A. objective (NPLAN EPI; Leica). Spectra were acquired in 100 s and processed using WiRE software.

Live Cell Imaging. HeLa cells were seeded on glass coverslips and cultured in DMEM with 10% (v/v) FBS and 1% penicillin/streptomycin (Invitrogen). For EdU imaging experiments, media were changed to FBS-free DMEM for 24 h to synchronize cell cycles. The media were then changed back to DMEM with 10% FBS at the time isotopically edited EdUs were added to media to a final concentration of 100 μM . Fifteen h later, the coverslips were washed with PBS and assembled into imaging chambers using imaging spacers (GBL 654008, Sigma) filled with PBS. For three-color imaging with EdU- ^{13}C , EU- $^{13}\text{C}_2$, and 17-ODYA, HeLa cells were synchronized by changing to FBS-free DMEM for 24 h, followed by incubating with DMEM (10% FBS) in the presence of 100 μM EdU- ^{13}C and 50 μM 17-ODYA. Nine h later, EU- $^{13}\text{C}_2$ was also added to the media (final concentration 2 mM). The cells were incubated for another 6 h before being washed with PBS and assembled into imaging chambers for SRS imaging.

ASSOCIATED CONTENT

Supporting Information

DFT calculation methods, additional synthetic procedure, characterization details. This material is available free of charge via the Internet at <http://pubs.acs.org>.

AUTHOR INFORMATION

Corresponding Authors

cn37@columbia.edu

wm2256@columbia.edu

Notes

The authors declare the following competing financial interest(s): Z.C., L.W., and W.M. are the inventors of a patent application filed by Columbia University. R.A.F. has an interest in Schrödinger, Inc. R.A.F. has a significant financial stake in Schrödinger, Inc., is a consultant to Schrödinger, Inc. and is on the Scientific Advisory Board of Schrödinger, Inc.

ACKNOWLEDGMENTS

We thank F. Hu, Y. Shen, and M. Jimenez for helpful discussions. D.W.P. and C.N. acknowledge support from the Chemical Sciences, Geosciences and Biosciences Division, Office of Basic Energy Sciences, U.S. Department of Energy (DOE) under award number DE-FG02-01ER15264. W.M. acknowledges support from NIH Director's New Innovator Award and Alfred P. Sloan Research Fellowship.

REFERENCES

- (1) Lavis, L. D.; Raines, R. T. *ACS Chem. Biol.* **2008**, *3*, 142.
- (2) Shaner, N. C.; Steinbach, P. A.; Tsien, R. Y. *Nat. Methods* **2005**, *2*, 905.
- (3) Michalet, X.; Pinaud, F. F.; Bentolila, L. A.; Tsay, J. M.; Doose, S.; Li, J. J.; Sundaresan, G.; Wu, A. M.; Gambhir, S. S.; Weiss, S. *Science* **2005**, *307*, 538.
- (4) Miyawaki, A. *Annu. Rev. Biochem.* **2011**, *80*, 357.
- (5) Donnert, G.; Keller, J.; Wurm, C. A.; Rizzoli, S. O.; Westphal, V.; Schöne, A.; Jahn, R.; Jakobs, S.; Eggeling, C.; Hell, S. W. *Biophys. J.* **2007**, *92*, L67.
- (6) Bates, M.; Huang, B.; Dempsey, G. T.; Zhuang, X. *Science* **2007**, *317*, 1749.
- (7) Zhao, Y.; Araki, S.; Wu, J.; Teramoto, T.; Chang, Y.-F.; Nakano, M.; Abdelfattah, A. S.; Fujiwara, M.; Ishihara, T.; Nagai, T.; Campbell, R. E. *Science* **2011**, *333*, 1888.
- (8) Yan, P.; Acker, C. D.; Zhou, W.-L.; Lee, P.; Bollensdorff, C.; Negrean, A.; Lotti, J.; Sacconi, L.; Antic, S. D.; Kohl, P.; Mansvelder, H. D.; Pavone, F. S.; Loew, L. M. *Proc. Natl. Acad. Sci. U. S. A.* **2012**, *109*, 20443.
- (9) Wei, L.; Yu, Y.; Shen, Y.; Wang, M. C.; Min, W. *Proc. Natl. Acad. Sci. U. S. A.* **2013**, *110*, 11226.
- (10) Yamakoshi, H.; Dodo, K.; Okada, M.; Ando, J.; Palonpon, A.; Fujita, K.; Kawata, S.; Sodeoka, M. *J. Am. Chem. Soc.* **2011**, *133*, 6102.
- (11) Yamakoshi, H.; Dodo, K.; Palonpon, A.; Ando, J.; Fujita, K.; Kawata, S.; Sodeoka, M. *J. Am. Chem. Soc.* **2012**, *134*, 20681.
- (12) Wei, L.; Hu, F.; Shen, Y.; Chen, Z.; Yu, Y.; Lin, C.-C.; Wang, M. C.; Min, W. *Nat. Methods* **2014**, *11*, 410.
- (13) Freudiger, C. W.; Min, W.; Saar, B. G.; Lu, S.; Holtom, G. R.; He, C.; Tsai, J. C.; Kang, J. X.; Xie, X. S. *Science* **2008**, *322*, 1857.
- (14) Saar, B. G.; Freudiger, C. W.; Reichman, J.; Stanley, C. M.; Holtom, G. R.; Xie, X. S. *Science* **2010**, *330*, 1368.
- (15) Min, W.; Freudiger, C. W.; Lu, S.; Xie, X. S. *Annu. Rev. Phys. Chem.* **2011**, *62*, S07.
- (16) Cheng, J.-X.; Xie, X. S. *Coherent Raman Scattering Microscopy*; CRC Press: Boca Raton, FL, 2012.
- (17) Liu, Z.; Li, X.; Tabakman, S. M.; Jiang, K.; Fan, S.; Dai, H. *J. Am. Chem. Soc.* **2008**, *130*, 13540.
- (18) Paul, C.; Wang, J.; Wimley, W. C.; Hochstrasser, R. M.; Axelsen, P. H. *J. Am. Chem. Soc.* **2004**, *126*, S843.
- (19) Dieringer, J. A.; Lettan, R. B.; Scheidt, K. A.; Van Duyne, R. P. *J. Am. Chem. Soc.* **2007**, *129*, 16249.
- (20) Etchegoin, P. G.; Le Ru, E. C.; Meyer, M. *J. Am. Chem. Soc.* **2009**, *131*, 2713.
- (21) Silverman, L. N.; Pitzer, M. E.; Ankomah, P. O.; Boxer, S. G.; Fenlon, E. E. *J. Phys. Chem. B* **2007**, *111*, 11611.
- (22) Lipkin, J. S.; Song, R.; Fenlon, E. E.; Brewer, S. H. *J. Phys. Chem. Lett.* **2011**, *2011*, 1672.
- (23) Fürstner, A. *Angew. Chem., Int. Ed. Engl.* **2013**, *52*, 2794.
- (24) Baker, J.; Jarzecki, A. A.; Pulay, P. *J. Phys. Chem. A* **1998**, *102*, 1412.
- (25) Salic, A.; Mitchison, T. J. *Proc. Natl. Acad. Sci. U. S. A.* **2008**, *105*, 2415.
- (26) Yu, C.-S.; Oberdorfer, F. *Synlett* **2000**, *2000*, 86.
- (27) Katz, T. J.; McGinnis, J. J. *Am. Chem. Soc.* **1975**, *97*, 1592.
- (28) Schrock, R. R. *Acc. Chem. Res.* **1986**, *19*, 342.
- (29) Haberlag, B.; Freytag, M.; Daniliuc, C. G.; Jones, P. G.; Tamm, M. *Angew. Chem., Int. Ed. Engl.* **2012**, *51*, 13019.
- (30) McCullough, L. G.; Listemann, M. L.; Schrock, R. R.; Churchill, M. R.; Ziller, J. W. *J. Am. Chem. Soc.* **1983**, *105*, 6729.
- (31) Fürstner, A.; Mathes, C. *Org. Lett.* **2001**, *3*, 221.
- (32) Wengrovius, J. H.; Sancho, J.; Schrock, R. R. *J. Am. Chem. Soc.* **1981**, *103*, 3932.
- (33) Hickmann, V.; Alcarazo, M.; Fürstner, A. *J. Am. Chem. Soc.* **2010**, *132*, 11042.
- (34) Jyothish, K.; Zhang, W. *Angew. Chem., Int. Ed. Engl.* **2011**, *50*, 3435.
- (35) Alfano, R. R.; Baldeck, P. L.; Ho, P. P.; Agrawal, G. P. *J. Opt. Soc. Am. B* **1989**, *6*, 824.
- (36) Grammel, M.; Hang, H. C. *Nat. Chem. Biol.* **2013**, *9*, 475.
- (37) Kolb, H. C.; Finn, M. G.; Sharpless, K. B. *Angew. Chem., Int. Ed. Engl.* **2001**, *40*, 2004.
- (38) Jao, C. Y.; Salic, A. *Proc. Natl. Acad. Sci. U. S. A.* **2008**, *105*, 15779.
- (39) Martin, B. R.; Cravatt, B. F. *Nat. Methods* **2009**, *6*, 135.
- (40) Heppekaussen, J.; Stade, R.; Goddard, R.; Fürstner, A. *J. Am. Chem. Soc.* **2010**, *132*, 11045.
- (41) Yang, H.; Liu, Z.; Zhang, W. *Adv. Synth. Catal.* **2013**, *355*, 885.
- (42) Paley, D. W.; Sedbrook, D. F.; Decatur, J.; Fischer, F. R.; Steigerwald, M. L.; Nuckolls, C. *Angew. Chem., Int. Ed. Engl.* **2013**, *52*, 4591.
- (43) Lin, Y. A.; Boutureira, O.; Lercher, L.; Bhushan, B.; Paton, R. S.; Davis, B. G. *J. Am. Chem. Soc.* **2013**, *135*, 12156.
- (44) Kurhanewicz, J.; Bok, R.; Nelson, S. J.; Vigneron, D. B. *J. Nucl. Med.* **2008**, *49*, 341.
- (45) Senyo, S. E.; Steinhauser, M. L.; Pizzimenti, C. L.; Yang, V. K.; Cai, L.; Wang, M.; Wu, T.-D.; Guerquin-Kern, J.-L.; Lechene, C. P.; Lee, R. T. *Nature* **2013**, *493*, 433.
- (46) Palonpon, A. F.; Ando, J.; Yamakoshi, H.; Dodo, K.; Sodeoka, M.; Kawata, S.; Fujita, K. *Nat. Protoc.* **2013**, *8*, 677.
- (47) Palonpon, A. F.; Sodeoka, M.; Fujita, K. *Curr. Opin. Chem. Biol.* **2013**, *17*, 708.
- (48) Xu, C.; Wise, F. W. *Nat. Photonics* **2013**, *7*, 875.
- (49) Zhang, D.; Slipchenko, M. N.; Leaird, D. E.; Weiner, A. M.; Cheng, J.-X. *Opt. Express* **2013**, *21*, 13864.
- (50) Kong, L.; Ji, M.; Holtom, G. R.; Fu, D.; Freudiger, C. W.; Xie, X. S. *Opt. Lett.* **2013**, *38*, 145.
- (51) Sletten, E. M.; Bertozzi, C. R. *Acc. Chem. Res.* **2011**, *44*, 666.
- (52) Debets, M. F.; van Berkel, S. S.; Dommerholt, J.; Dirks, A. T. J.; Rutjes, F. P. J. T.; van Delft, F. L. *Acc. Chem. Res.* **2011**, *44*, 805.
- (53) Devaraj, N. K.; Weissleder, R. *Acc. Chem. Res.* **2011**, *44*, 816.
- (54) Agard, N. J.; Prescher, J. A.; Bertozzi, C. R. *J. Am. Chem. Soc.* **2004**, *126*, 15046.
- (55) Blackman, M. L.; Royzen, M.; Fox, J. M. *J. Am. Chem. Soc.* **2008**, *130*, 13518.